6. Comparative study on galling and antiwear behaviour of polyurethane based coatings reinforced with pristine and alkylated MoS_2 nanosheets.

**Work accepted in ASME Journal of Tribology*

This chapter is focused on tribological studies of polyurethane (PU) based coatings doped with nano-MoS_2, and MoS_2 functionalized with octadecanethiol (i.e., MoS_2-ODT) on steel substrate. The high-resolution transmission electron microscopy (HRTEM) confirmed that the MoS_2 nanosheets contain few layers and are made up of 3-10 molecular thick lamellae. The Fourier transform infrared radioscopy (FTIR) results of nanosheets confirmed the functionalization of MoS_2 nanosheets with ODT, and XRD of the nanosheets confirmed that the crystal structure of MoS_2-ODT nanosheets was not affected by the addition of ODT. Tribological tests were carried out under two contact conditions, i.e., sliding contact for galling resistance and reciprocating wear studies. The PU-based nanocomposite coatings showed enhanced galling resistance at room temperature. The reciprocating wear studies showed a significant reduction in friction and wear with the addition of MoS_2 and MoS_2-ODT nanosheets in the polymer matrix. The PU-based nanocomposite coatings showed up to 77 and 95% reduction in coefficient of friction and wear, respectively.

6.1. Introduction.

The polymer coatings can achieve low friction and wear in dry and lubricated tribological conditions. The polymer coatings are used for various industrial applications (automobiles, bearings, food conveyors, and semiconductors) because of their low cost, corrosion resistance, biocompatibility, and self-cleaning properties [49,201,293–295]. Moreover, the mechanical and tribological properties of polymeric materials can be enhanced significantly with the addition of nano and micro-size fillers into the polymer matrix. Various filler materials like

silica nanoparticles, MoS_2 nanosheets, carbon nanotubes, titanium dioxide nanoparticles, etc., have been used as fillers with different polymers to enhance their mechanical and tribological properties [45,48,60,296–298]. The weak Vander wall forces between the layers of MoS_2 nanosheets allow them to easily shear over each other, making them good candidates for boundary lubrication conditions [299]. The nanosized MoS_2 particles have shown better tribological properties than bulk ones [300]. The friction and wear properties of MoS_2 greatly depends on its morphology, such as nanoballs, nanotubes, nanosheets, etc. [299–301]. The MoS_2 nanosheets easily penetrate between the tribopairs and provide better lubrication than the nanoballs [300]. The MoS_2 nanosheets undergo triboinduced exfoliation and deformation, resulting in the formation of thin film on the rubbing surfaces with low shear strength and helping to improve tribological properties [299–302]. Polymer coatings can be used in both lubricated and unlubricated conditions. Since there are many constraints in liquid lubrication, the study of polymer-based coatings is imperative for various tribological applications.

Polyurethane (PU) based polymer coatings have been widely explored for tribological studies because of being anti-corrosive, abrasion, and erosion resistant properties [42,44,46,198,293,303–306]. They have also been used with various filler elements, which includes ionic liquids, silica gel, polyethylene wax, graphene, epoxy, and many more [307–310]. The PU based coatings show good adhesion to the substrates and are lighter than their metallic or ceramic counterpart. All these properties of PU based coatings, along with their cost-effectiveness, also make them an important constituent of bioactive composites [311]. Hence the PU based coatings have found their use in a vast number of applications.

Galling has been a limiting factor for many tribosystems containing dry sliding tribopairs. Galling majorly occurs when the sliding speed is low, and the contact pressure is high. The surface protrusions formed during galling due to plastic deformation, material transfer, or both are much worse than any other form of wear. The tribopairs which form strong adhesive bonds

during sliding (like stainless steel) are more prone to galling. Therefore, mitigation of galling under tribological contact conditions is very important. Several researchers have reported that coating with different kinds of ceramic (TiN, CrN, DLC, CrC, etc.) can enhance the galling resistance of a surface [250,271,290,292]. However, very little literature is available on the galling resistance of polymeric materials [269,312]. The literature suggests that polymers like polytetrafluoroethylene (PTFE) and polyamides possess good lubricating properties because of their viscoplastic or plastic properties. These polymers possess better thermal stability than other commercially available polymers, and at high temperature PTFE reacts with the metal substrate to form a thin lubricating fluoride. Hence, making them good candidates for the coatings having good galling resistance. However, creating composite coatings of polyamide and PTFE is very difficult. Due to the high thermal stability of these polymers, sophisticated thermal spray setup is needed to coat them on substrates. Therefore, for creating composite coatings of these polymers at laboratory scale, PTFE's nano and micro size particles have been used as fillers for epoxy and nickel based coatings to improve galling resistance [313,314].

As mentioned in the previous chapter, ASTM G98 and G196 are the standards researchers use for galling tests [6,7]. **Table** 6.1 summarizes the standards used by various researchers to ascertain the galling behaviour of different materials. From **Table** 6.1, it is evident that very few researchers have reported about galling behaviour of polymer based coatings according to ASTM G98 and G196 to study the galling resistance of the material pairs. ASTM G98 and G196 have advantages and disadvantages, as mentioned in the previous chapter.

MoS_2 nanosheets have been widely used as fillers for different polymer matrices [46,304,315]. The present work focuses on developing pristine and alkylated MoS_2 nanosheets through a hydrothermal process followed by Rawat et al. [213]. The MoS_2 nanosheets contained a few layers (3-10) and had an ultrafine thickness (2.5-7 nm) with a length of less than 100 nm. Various researchers have mentioned that MoS_2 nanosheets show good tribological properties

in a polymer matrix around 2-3 wt% [47,60,304,315,316]. PU based coatings were prepared with 2 wt% of pristine and alkylated MoS_2 nanosheets. The friction and wear studies of the coatings were done through a reciprocating test rig. At the same time, the galling studies were done on the mechanized test rig developed by Harsha et al. [317], complying with the ASTM G196. In the present chapter, the authors have tried to improve the tribological properties (reciprocating and galling wear) of PU based coatings with the incorporation of pristine and alkylated MoS_2 nanosheets. The other researchers had also used similar functionalized MoS_2 (alkylated MoS_2) nanosheets in oil and lithium-based grease [213,318], but these nanosheets have never been explored with polymers. As shown in **Table** 6.1, very few literature is available on improving the galling resistance with the help of polymer coatings. In the present study, the authors have reported a cost-effective method of reducing galling at room temperature through PU based nanocomposite coatings, and also how the functionalization of MoS_2 nanosheets helps in improving the tribological performance of PU based nanocomposite coatings. These coatings can be used in food processing, medical and cold forming industries to improve the galling resistance of machine parts.

Table 6.1. Summary of work reported on galling over the years.

Authors and Reference	Standard for galling test	Coating	Important observations
Srinivasan et al. [314]	--	Ni/PTFE	• Incorporation of PTFE resulted in reduce wear. • Incorporation of PTFE does not affect corrosion behaviour of Ni.
Meng et al. [313]	--	Epoxy/PTFE	• The coating showed reduced friction and wear with greatly reduced adhesive wear. • The coating prevented galling of threaded oil couplings.
Raymond et al. [64]	--	Ag/PTFE	• The coating helped in preventing catastrophic screw thread failure by preventing the galling damage in the screw threads.
Hung et al. [63]	--	Ni-P/PTFE	• The adhesive damage decreased with increase in concentration of PTFE particles. • The hardness of the coating increased at higher temperature, but had a rudiment effect on galling performance.

6.2. Materials and methods.

6.2.1. Synthesis and functionalization of MoS_2 nanosheets.

A detailed explanation for preparation of MoS_2 and MoS_2-ODT nanosheets has already been explained in chapter 3. A schematic representation of the preparation of MoS_2 and MoS_2-ODT nanosheets has been provided in Figure 6.1 for a quick overview of the synthesis process.

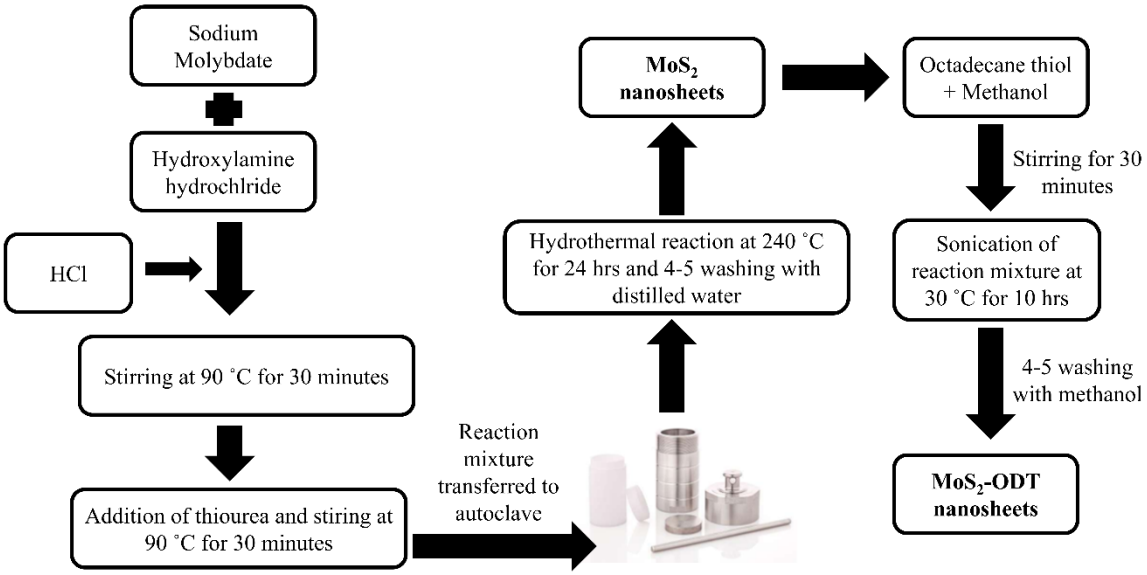

Figure 6.1. Schematic representation of MoS_2 and MoS_2-ODT nanosheets preparation.

2.2. Characterization of MoS_2 and MoS_2-ODT nanosheets.

The phase distribution and crystal structure of the nanosheets were analyzed by X-Ray diffractometer (SmartLab, Rigaku Corporation) with Cu K_α radiation in the 2Θ range of 10˚–80˚ and a grazing angle of 2˚. The nanostructural features of the pristine and alkylated nanosheets were studied with the help of high resolution transmission electron microscopy (HR-TEM, Tencnai G2 20 TWIN). Fourier transform infrared spectroscopy (FTIR, Nicolet iS5, Thermo Electron Scientific Instruments LLC) studies confirmed the functionalization of

long alkyl chains on MoS_2 nanosheets. The FTIR spectra were recorded in the spectral range of 400-3000 cm^{-1} with a resolution and scan rate of 4 cm^{-1} and 40, respectively.

6.2.3. Preparation of PU based nanocomposite coatings.

With its thinner and hardener, PU was procured from a commercial supplier having a glass transition temperature of -20 ˚C and melting point of 110 ˚C. The ratio of PU and hardener used was 3:1. The PU coatings were deposited on a SS 304 (25 X 25X 5 mm) and silicon substrates. The coatings were deposited through spray pyrolysis (Spray Pyrolysis Equipment, Holmarc). The samples were placed on a hot copper plate at 60˚C, and the polymer solution was sprayed through the syringe pump with the help of compressed air. The flow rate of the polymer solution was kept at 1500 µl/min. A total of four coats were deposited on the substrates, and the coated substrates were left inside the chamber on the heated plate for curing. Similarly, the PU based nanocomposite coatings were developed by spraying a solution of PU-MoS_2 and PU-MoS_2-ODT. The solutions for nanocomposite coatings were prepared by mixing 2 wt% nanosheets in PU. The galling samples were machined from hexagonal SS304 rod and prepared according to the ASTM G196 standard. The roughness of samples for reciprocating and galling tests was maintained at around 0.4 µm for better adhesion of the polymeric coating. **Figure** 6.2 shows the typical images of PU coated samples for reciprocating wear and galling tests.

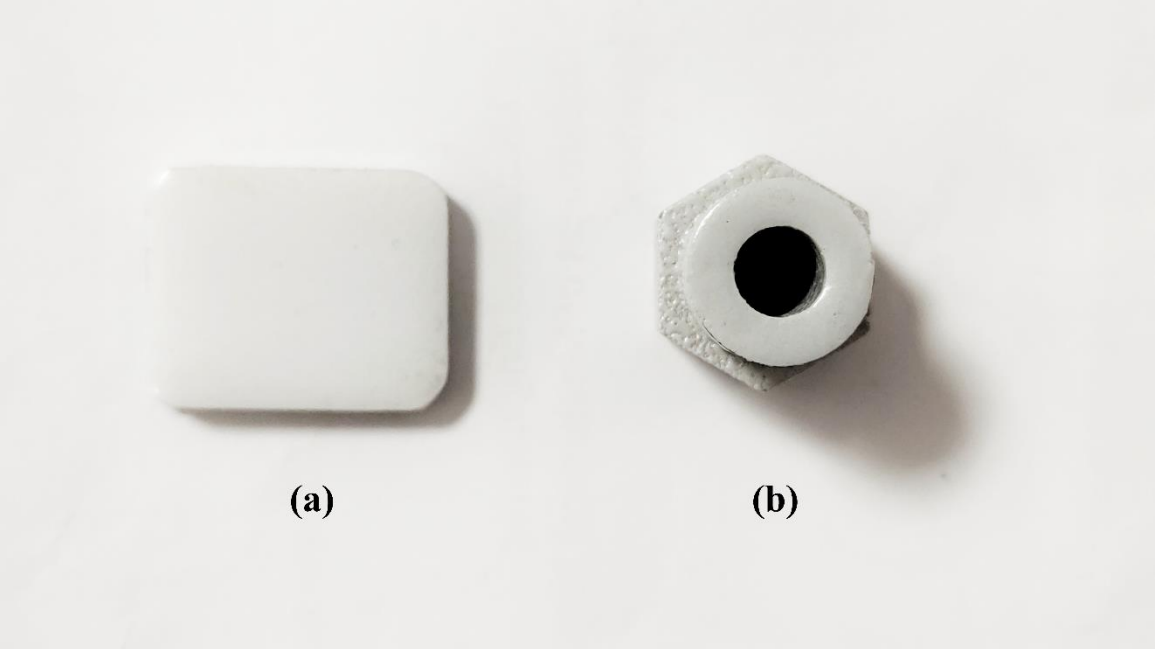

Figure 6.2. PU coated substrates for (a) reciprocating wear tests, and (b) galling tests.

6.2.4. Characterization of PU based nanocomposite coatings.

High-resolution scanning electron microscope (HRSEM) (Nova Nano SEM 450, FEI PTE LTD.) was used to study the cross-sectional morphology of the coating. The silicon substrate was cut, and the cross-section of the substrate was polished before analysis. The HRSEM has an energy dispersive spectroscopy (EDS) feature coupled with it. The EDS elemental mapping was used to study the dispersion of nanosheets in the polymer matrix. The hardness measurement of the coating was done with the help of a nanoindentation hardness tester (CSEM). A Berkovich diamond indenter having a displacement resolution of 0.04 nm and a force resolution of 0.04 μN was used for testing. The maximum load applied on the indenter was 5mN with a loading rate of 10mN/min and 2 seconds hold at maximum load. A total of 8 indentations were made to calculate the hardness and elastic modulus values through the Oliver Pharr method [214]. A nanoscratch tester (CETR-UMT) was used for scratch testing. The nanoscratch tester was equipped with a 200 μm tip radius Rockwell type of indenter. The load

was increased from 0 to 30 N at a loading rate of 0.5 N/sec and a scratch speed of 0.1 mm/sec. The critical scratch load was calculated from the peaks observed in acoustic emission data. The surface energy and water contact angle were measured with the help of a Goniometer.

6.2.5. Tribological characterization of PU based nanocomposite coatings.

A multifunctional tribometer (MFT, Rtech Instruments) was used for reciprocating testing. A 5 mm 100Cr6 bearing steel ball was used and the applied normal load was varied from 10 – 30 N. The sliding frequency of 5 Hz and a stroke length of 5mm was applied to the reciprocating arm (corresponding to the sliding velocity of 50mm/sec). The reciprocating tests were conducted for 1 hour (or 9000 cycles). The worn out areas were analyzed through a stereo-zoom microscope, and a contact type profilometer (INTRA, Taylor Hobson) was used to calculate the wear volume of the worn out profiles [215]. Then, the specific wear rate K (mm^3/Nm) was calculated as:

$$W_{\text{l,flat}} \approx R' - \sqrt[2]{R'^2 - \frac{{d_\text{p}}^2}{4}} \tag{6.1}$$

$$W_\text{q} \approx \frac{{d_\text{p}}^3}{12R'} \tag{6.2}$$

$$\Delta\text{V} \approx \frac{\pi {d_\text{p}}^2 W_{\text{l,flat}}}{8} + \Delta x W_\text{q} \tag{6.3}$$

$$\text{K} = \frac{\Delta\text{V}}{\text{LS}} \tag{6.4}$$

where R' is the radius of curvature (approximate) of the wear profile obtained through fitting the profile in the software of the profilometer. d_p is the width of wear scar perpendicular to the sliding direction. W_q is the planimetric wear and $W_{l,flat}$ is the linear wear of flat surface of the ball. ΔV corresponds to the total volume loss, L is the applied load, and S is the total sliding distance. **Figure** 6.3 represents the schematic representation of all the parameters required to

calculate the specific wear volume of the polymer coating. The wear analysis was only done for the coating as no wear was observed on the countersurface after the tribotesting. The manuscript discusses the relative change in wear across the deposited PU based nanocomposite coatings.

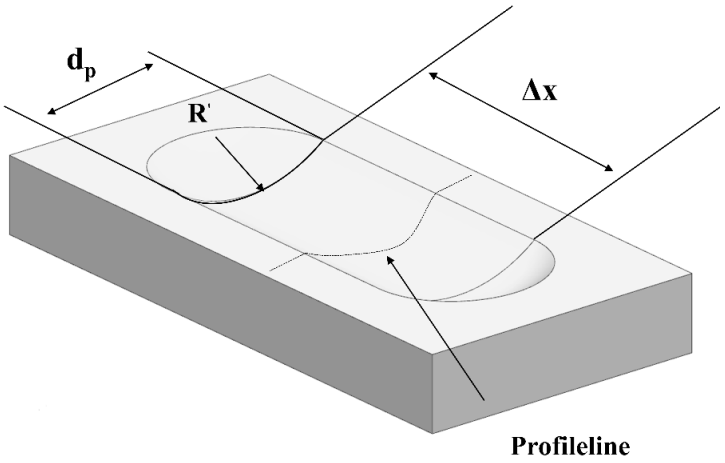

Figure 6.3. Schematic representation of parameters required to calculate specific wear volume of PU based coatings.

A galling test rig (Galling tester, DUCOM Instruments) was used for galling tests. The galling samples were machined from SS 304 rods according to ASTM G196 test geometry. The schematic diagram and description of the test rig have already been provided in chapter 3. The tests were conducted at room temperature, and the load was varied between 500 to 1750 N (corresponding contact pressure of 5 to 17.5 MPa). The rotation speed was 6 rpm, corresponding to a 3 mm/sec of average sliding velocity. The tests at each load were conducted till large fluctuations were observed in the friction torque data. The tests were stopped at the load on which the sample failed within one rotation (i.e., 10 seconds). To confirm the accuracy of the results, each test was repeated 5 times. The wear tracks of the PU based coatings of both the reciprocating and galling experiments were analyzed with the help of optical and stereo zoom microscopes.

6.3.1. Characterization of MoS2 and MoS2-ODT nanosheets.

The HRTEM images shown in **Figure** 6.4 depicts that the MoS_2 nanosheets contain few layers and are made up of 3-10 molecular thick lamellae. The thickness of the nanosheets varied from 2.5-7 nm with an interlamellar spacing of approximately 0.63 nm, which is quite close to the characteristic interlamellar spacing of the (002) plane of MoS_2, i.e., 0.62 nm. After the functionalization of the nanosheets with ODT, no change in interlamellar spacing was observed. Hence, the ODT molecules tethered only on the surface sites and did not attach in between nanosheets layers. The HRTEM images also did not show any nanostructural changes after the functionalization of the nanosheets.

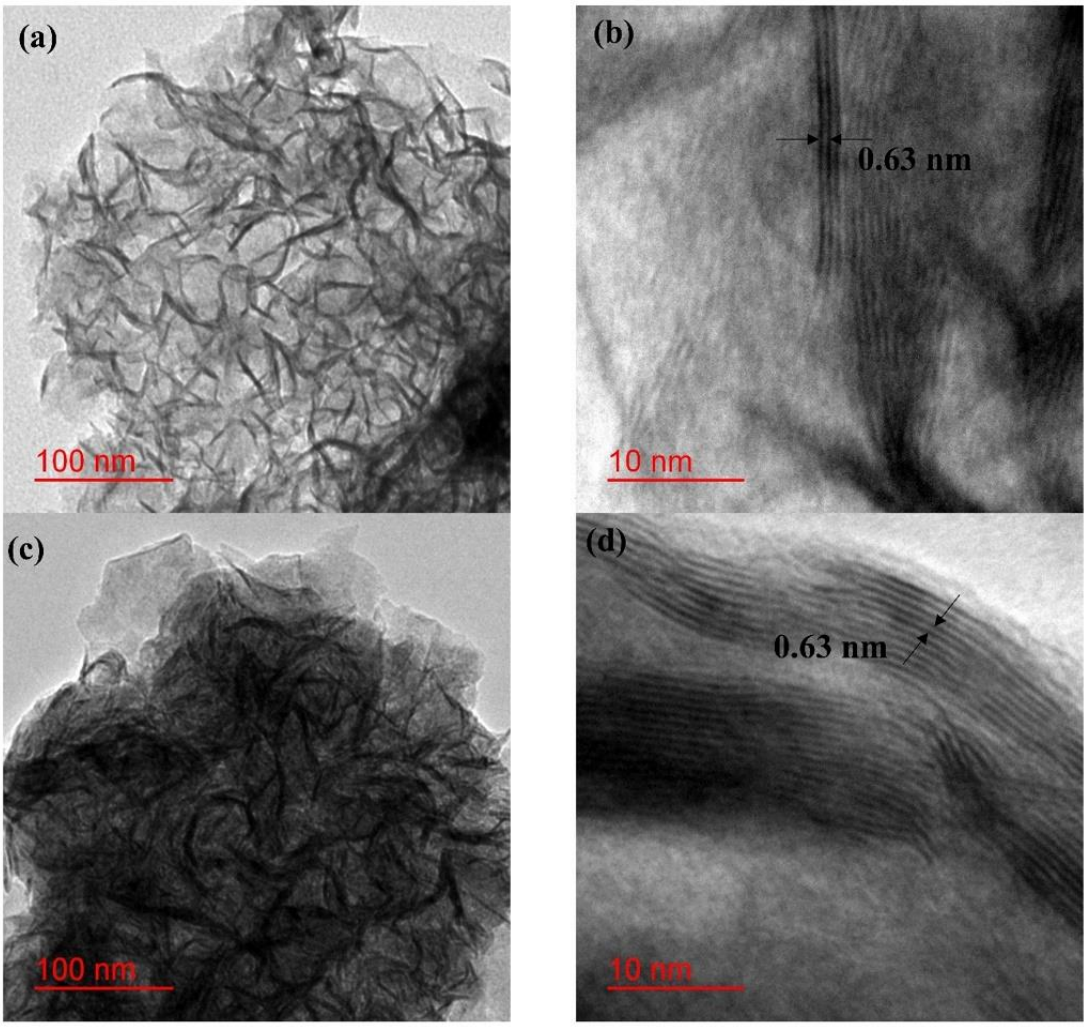

Figure 6.4. HRTEM images of (a) and (b) MoS_2, (c) and (d) MoS_2-ODT nanosheets.

Figure 6.5 shows the XRD peaks of MoS_2 and MoS_2-ODT nanosheets over the 2Θ range of 10˚ to 80˚. The MoS_2 diffraction peaks obtained at 2Θ = 14.12˚, 32.9˚, 39.5˚, 58.7˚, and 69.4˚ corresponding to (002), (101), (103), (110), and (201) planes, respectively. The peaks were in agreement with the peaks of MoS_2 from ICDD reference pattern 01-075-1539. The MoS_2 nanosheets belonged to a hexagonal crystal system with $P6_3/mmc$ space group. The peaks corresponding to MoS_2 in the diffraction pattern of MoS_2-ODT remained at the same position. Therefore, the crystal structure of MoS_2 was not affected after the functionalization with ODT. Several sharp peaks (unmarked) were observed in the diffraction pattern of MoS_2-ODT besides the MoS_2 diffraction peaks. These peaks were also observed by earlier researchers [213,318], but no description of these peaks was given. However, on comparing these peaks with the ICDD database, it was found that all peaks matched the diffraction peaks of sulphur (ICDD reference pattern 01-071-0396). The peaks may have arisen because of the presence of sulphur atoms in the thiol group used to functionalize MoS_2. Azzam et al. [319] also found the presence of these peaks while functionalizing silver nanoparticles with dodecane thiol.

The FTIR spectroscopy graphs shown in **Figure** 6.6 further confirms the functionalization of MoS_2 with ODT. A strong vibrational peak was obtained around 1650 cm^{-1}, which is associated with the bending mode of water molecules. The water gets absorbed in the defect sites of MoS_2, which are produced during the hydrothermal process [318]. The strong vibrational features arising between 2800-3000 cm^{-1} in MoS_2-ODT nanosheets (**Figure** 6.6(a)) are associated with methylene and methyl asymmetric and symmetric stretching modes (d^-, d^+, r^-, r^+) [318]. These vibrational features reveal the functionalization of MoS_2 nanosheets with ODT. Also, the vibrational features at 1468 and 718 cm^{-1} are due to rocking and scissor modes of methylene units of functionalized MoS_2 sheets with ODT [213]. The vibrational features present at 472 cm^{-1} in **Figure** 6.6(b) are ascribed to the Mo-S stretching [213].

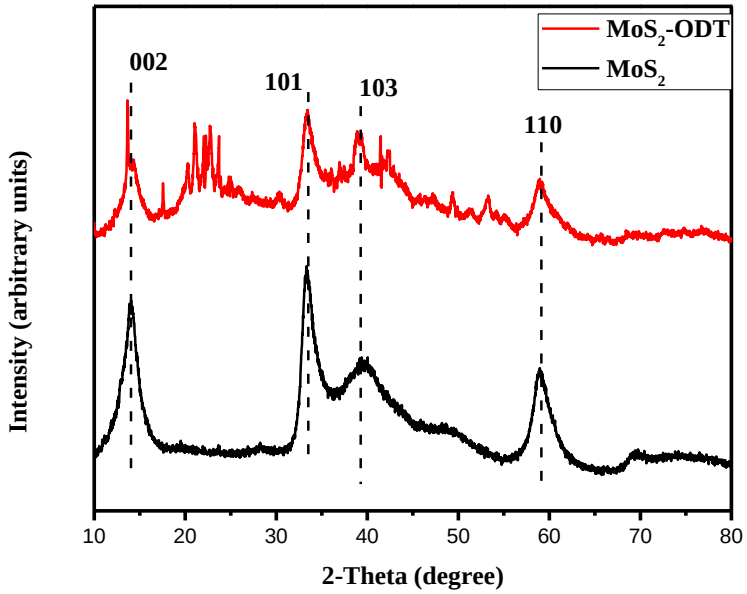

Figure 6.5. XRD data of MoS_2 and MoS_2-ODT nanosheets.

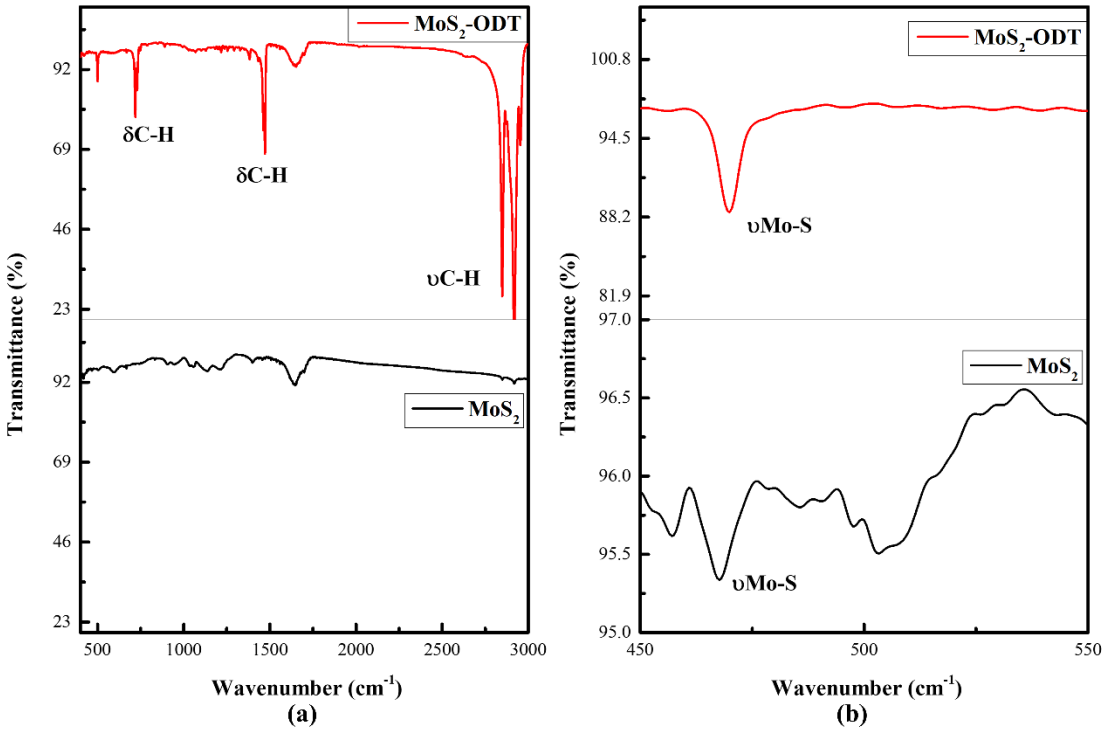

Figure 6.6. FTIR spectra of MoS_2 and MoS_2-ODT nanosheets.

6.3.2. Characterization of PU based nanocomposite coatings.

The cross-sectional SEM images of the PU-MoS_2 and PU-MoS_2-ODT coatings are shown in **Figures** 6.7(a) and (b). The thickness of the coating deposited varied between 450-500 µm. The EDS elemental mapping of the molybdenum (Mo) atom was used to study the dispersion of nanoparticles in the polymer matrix. As observed from the elemental mapping of Mo in PU-MoS_2 coating (**Figure** 6.7(c)), the nanosheets have a good dispersion but also showed signs of agglomeration. In contrast, the nanosheets in PU-MoS_2-ODT coating showed excellent dispersion with negligible signs of agglomeration. Therefore, the functionalization of MoS_2 nanosheets with ODT helped in the proper dispersion of MoS_2 nanosheets in the polymer matrix.

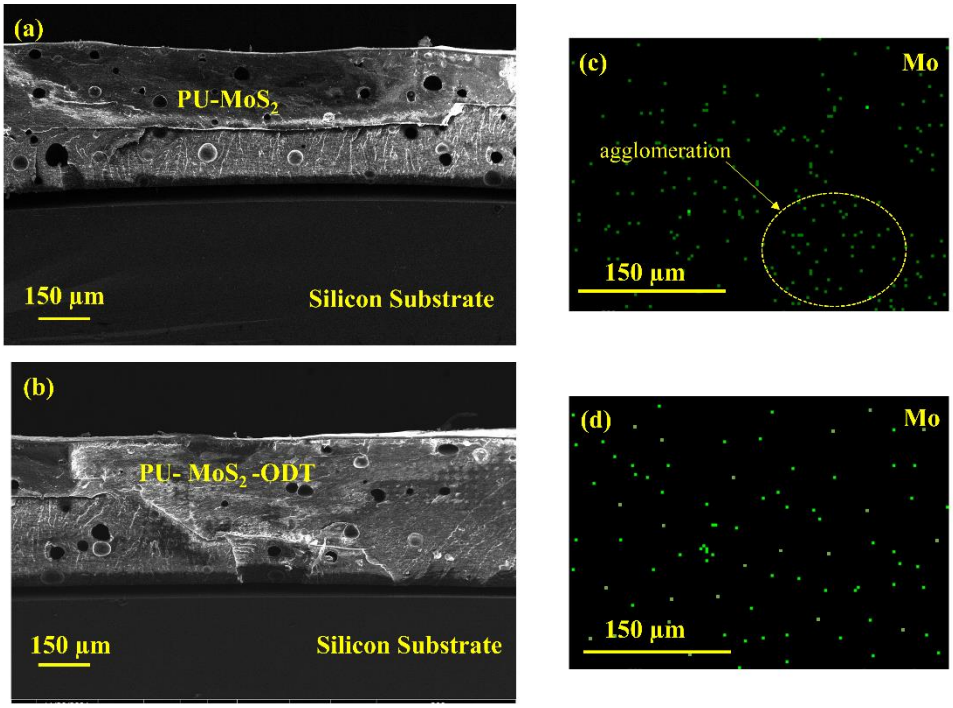

Figure 6.7. SEM images of cross-section of the (a) PU-MoS_2, (b) PU-MoS_2-ODT coatings; Elemental mapping of Mo in (c) PU-MoS_2, (d) PU-MoS_2-ODT coatings.

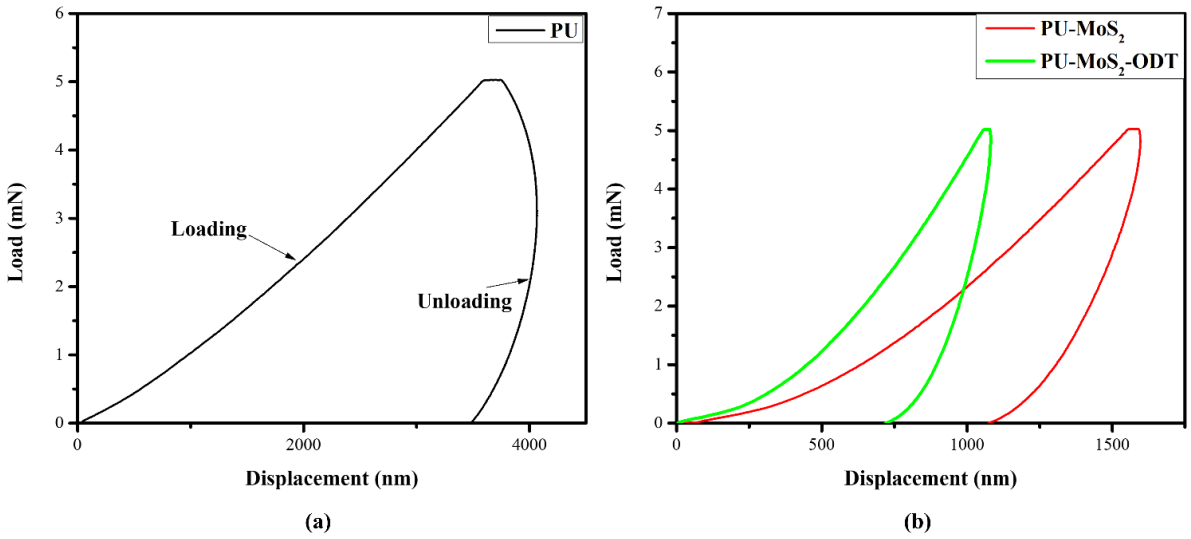

Figure 6.8. Nanohardness loading and unloading curves of (a) plain PU, (b) PU-MoS_2, and (c) PU-MoS_2-ODT coatings.

The hardness of the polymer composite coatings was measured by nanoindentation. **Figure** 6.8 shows the load-displacement curves for the three coatings tested under nanoindentation. Due to the high recovery rate of plain PU coating, the hardness of the coating remains undetermined. The Oliver Pharr method [214] uses the slope of the initial values of the unloading curve to calculate the elastic modulus of the substrate. For the plain PU coating, the unloading curve showed unusual bulging during the unloading cycle, and the indenter moved further inside the coating even after removing the load. This is due to the residual strain formation in the elastomeric compounds when subjected to stresses [320]. The softer the material, the longer the time it takes to recover the residual strain. The unusual bulging in the plain PU based coating resulted in the negative slope of the initial values of the unloading curve (**Figure** 6.8(a)), due to which the software was unable to estimate the hardness and elastic modulus of the plain PU coating. However, a comparative hardness estimation can be made by observing the loading curves of each coating in **Figure** 6.8, as the hardness of the substrate is indirectly

related to the maximum penetration depth in the Oliver Pharr method [214]. The maximum penetration depth of the indenter in the plain PU coating is about 3 and 4 times the maximum penetration depth in the PU-MoS_2 and PU-MoS_2-ODT coatings, respectively. This signifies that the addition of MoS_2 nanosheets helped in strengthening the PU matrix, and the less residual strain was developed in the coatings containing MoS_2 nanosheets. A similar kind of observation was also confirmed by Neha et. al.[321], while adding MoS_2 in the matrix of ultra-high molecular weight polyethylene and epoxy. The PU-MoS_2-ODT coating showed an even better hardness value than PU-MoS_2 coating. This can be attributed to the presence of sulphur in MoS_2-ODT nanosheets (as observed from the XRD results in **Figure** 6.5**)**, which helps in better crosslinking in thermosetting polymers [322], and hence better hardness.

The surface energy of the polymer surface was calculated through two liquid method [60]. The data in **Table** 6.2 shows that the contact angle of water with the surface increases after the addition of MoS_2 nanosheets. When MoS_2-ODT nanosheets are added, the contact angle increases even more. This is because of the hydrophobic nature of ODT [323]. PU coatings are known for their smooth and glossy finish and have low roughness (**Table** 6.2). A slight increase in roughness was observed with the addition of MoS_2 and MoS_2-ODT nanosheets. However, all the roughness values were still within the range of 0.2 µm, which is necessary for good tribological properties.

The adhesive strength of the PU based coatings was analyzed by a scratch test. In general, the evaluation of the scratch test is based on analysis of data related to load, time or depth, and microscopic analysis of the scratch groove. For polymer coatings, it was challenging to locate the initial failure load of coatings through microscopic analysis of the scratch groove as polymers have a good elastic recovery rate. Therefore, the lower load at which the coatings might have failed gets masked with the recovery of polymer in that region. Hence many researchers calculate the scratch hardness or plowing hardness [324]. Whereas, the acoustic

emission data recorded during scratch testing of polymer coatings can give a better understanding of the load at which the coating failure occurs. The acoustic emission data and

Table 6.2. Various properties of PU based nanocomposite coatings.

Properties	PU	PU-MoS_2	PU-MoS_2-ODT
Hardness (MPa)	-	170	267
Elastic Modulus (GPa)	-	3.45	4.2
H/E	-	0.05	0.07
Contact angle with DI water	68˚	78˚	83˚
Contact angle with n-hexane	15˚	18˚	20˚
Surface Energy (N-m)	0.028	0.025	0.020
Roughness	0.09 µm	0.13 µm	0.16 µm

the optical microscopic images of scratches of PU based coatings are shown in **Figures** 6.9 and 6.10. As seen in **Figure** 6.9, the spikes in the acoustic emission data show the load at which the indenter hits the steel substrate, and the adhesive bond between the coating and the steel substrate is broken. The plain PU coating failed at 16.7 N, while the PU-MoS_2 and PU-MoS_2-ODT coatings failed at 20.7 and 22.5 N loads, respectively. The higher scratch-resistance of the PU-MoS_2 and PU-MoS_2-ODT coatings is due to the enhanced hardness of these coatings by incorporating MoS_2 and MoS_2-ODT nanosheets, respectively. Since the elastic modulus value of plain PU coating was not deduced through nanoindentation testing, so the Hertzian contact stress corresponding to 16.7 N load was undetermined. The Hertzian contact stresses corresponding to 20.7 and 22.5 N load for the PU-MoS_2 and PU-MoS_2-ODT coating are 1.8 and 2.2 GPa, respectively.

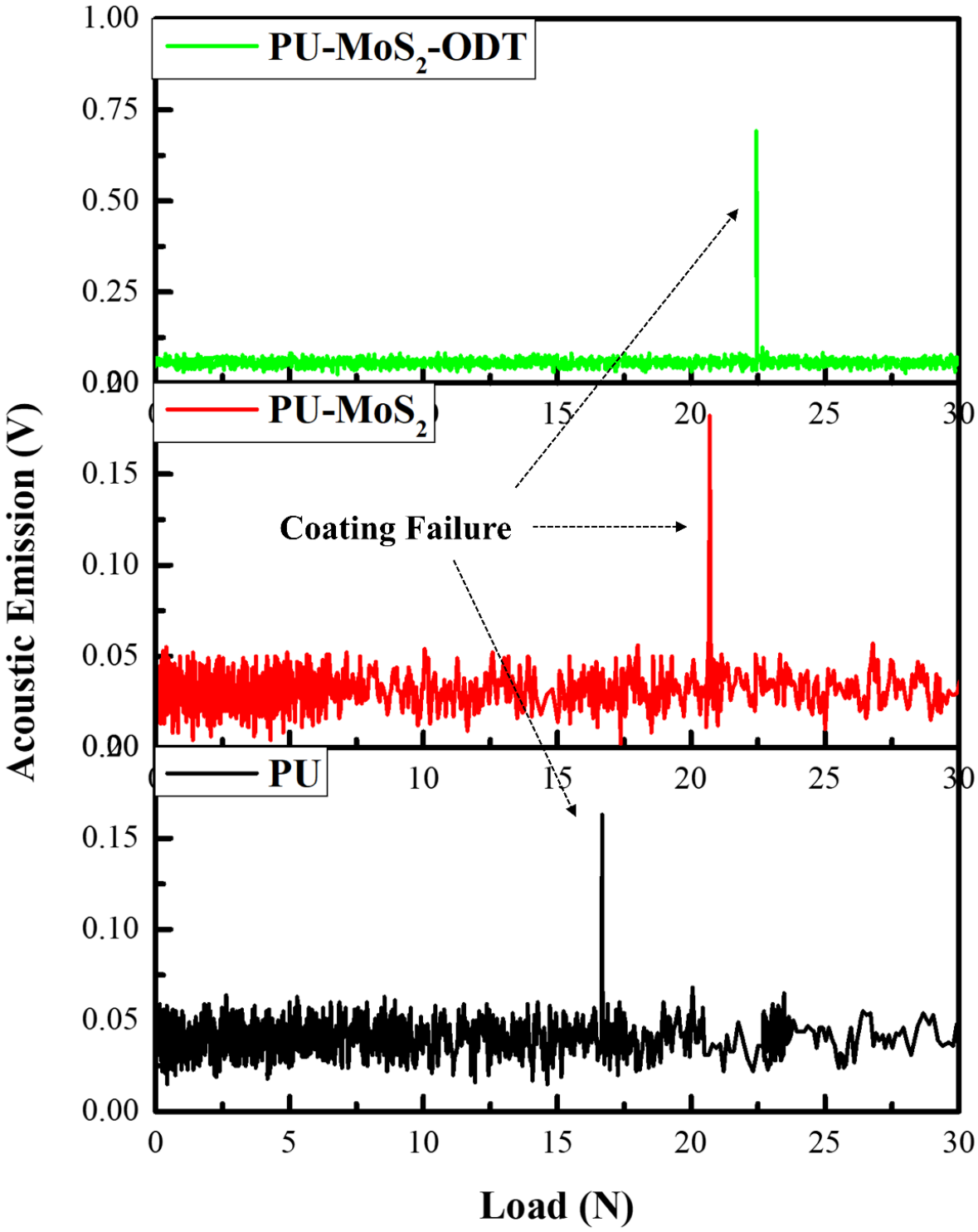

Figure 6.9. Acoustic emission data of the scratch test of PU based coatings.

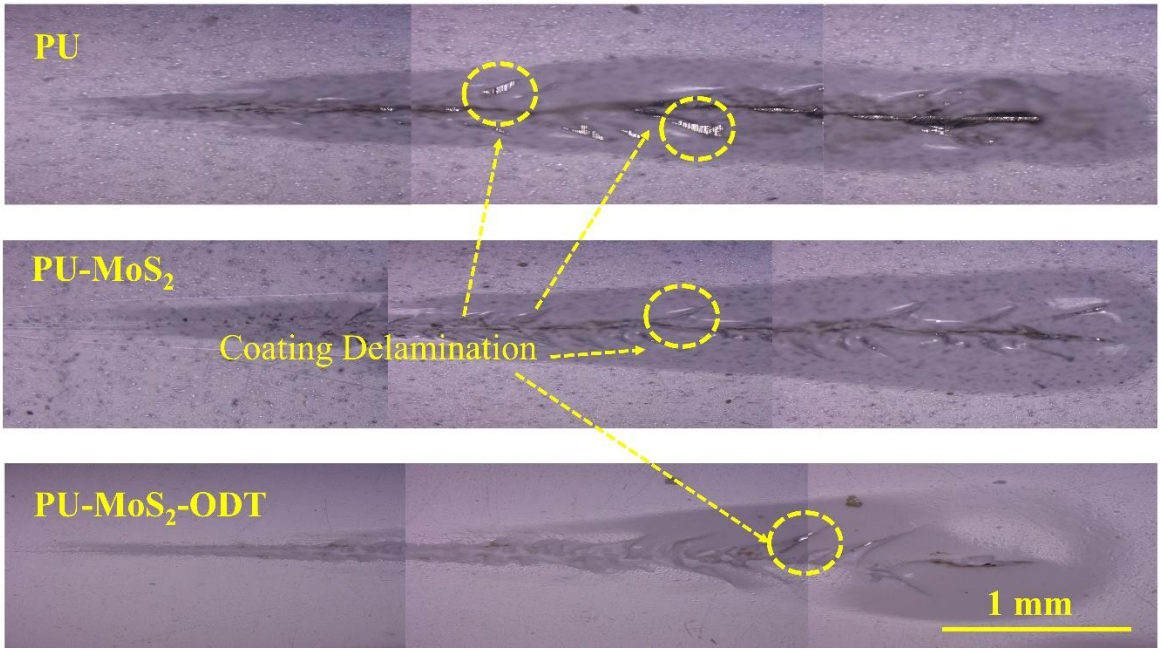

Figure 6.10. Optical microscopic images of scratches of PU based coatings.

6.3.3. Tribological characterization of PU based nanocomposite coatings.

6.3.3.1. Reciprocating friction tests.

Figure 6.11 shows the coefficient of friction curves for each polymer coating. At 10 N load (**Figure** 6.11(a)), the steady state coefficient of friction obtained was about 0.65. Whereas, after the addition of MoS_2 nanosheets, the steady state coefficient of friction dropped to 0.35. The PU-MoS_2 coating reduced the coefficient of friction by 46%. The lamellar structure of MoS_2 sheets and the weak Vander Walls forces between the MoS_2 layers helped in reduce the friction coefficient. However, the PU-MoS_2-ODT coating observed more reduction in coefficient of friction than PU-MoS_2 coating. The steady state coefficient of friction was 0.15, approximately 77% reduction from the plain PU coating. The low surface energy of PU-MoS_2-ODT coating (**Table 2**) helped in lowering the coefficient even more than PU-MoS_2 coating. The low surface energy indicates lower adhesive forces on the surfaces of the PU based nanocomposite coatings. Therefore, both PU-MoS_2 and PU-MoS_2-ODT coatings experienced a lower

coefficient of friction than the plain PU coating. Furthermore, the running-in period of PU-MoS_2-ODT coating was lower than PU-MoS_2 coating, which indicates that the functionalization of MoS_2 nanosheets with ODT helped in early tribofilm formation. At higher load of 20 N (**Figure** 6.11(b)), the plain PU and PU-MoS_2 coatings failed after 570 and 1100 seconds, respectively. A continuous decrease in the friction curve can be seen after 570 and 1100 seconds in plain PU and PU-MoS_2 coating, respectively, when tested at 20N. The entire ball collet rested on the polymer surface when the coating failed. This led to a decrease in the stress exerted on the coating surface, and the coefficient of friction started dropping. Whereas the PU-MoS_2-ODT coating showed a steady state friction coefficient of 0.20 at 20 N. The PU-MoS_2-ODT coating observed a slight increase in the coefficient of friction at 20 N (**Figure** 6.11(c)) due to the formation of more wear debris at higher loads. At the same time, the coating failed after 1000 seconds when it was tested at a 30 N load.

Table 6.3. Maximum Hertzian contact stress for PU-MoS_2 and PU-MoS_2-ODT coatings at various loads.

	PU-MoS_2	PU-MoS_2-ODT
Maximum Hertzian Contact Stress at 10 N (MPa)	165	190
Maximum Hertzian Contact Stress at 20 N (MPa)	208	239
Maximum Hertzian Contact Stress at 30 N (MPa)	239	275

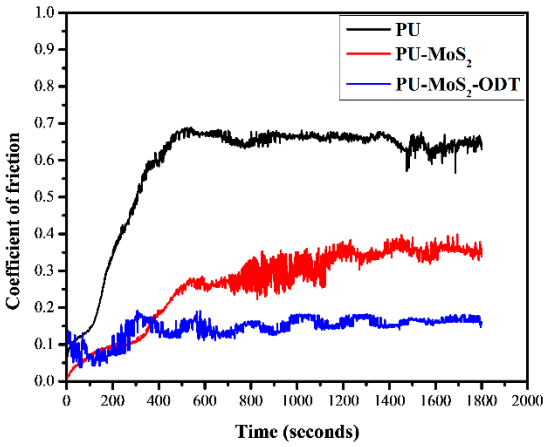

(a)

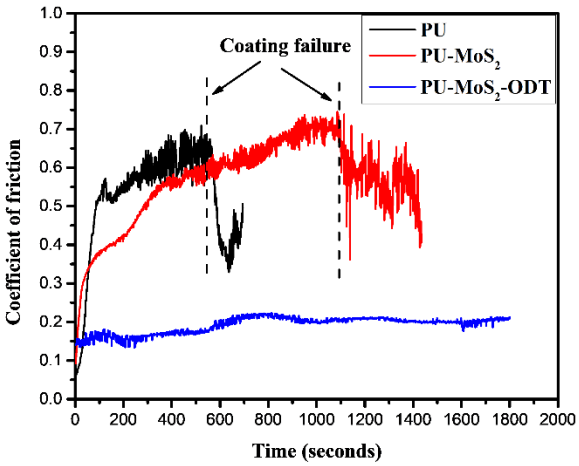

(b)

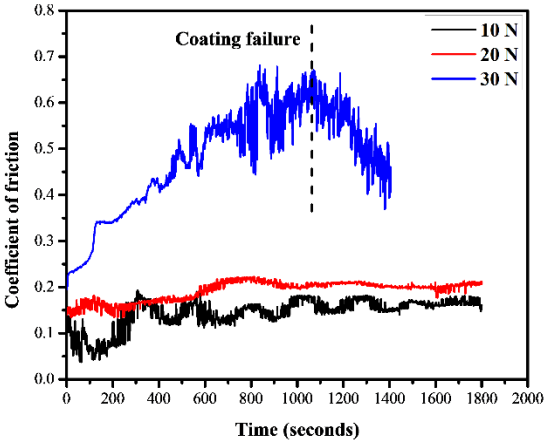

(c)

Figure 6.11. Coefficient of friction curves for (a) PU based nanocomposite coatings at 10 N, (b) 20 N, and (c) PU-MoS_2-ODT coating at different loads.

Figure 6.12(a) depicts the wear profiles of various polymers tested at 10 N under reciprocating friction tests. The plain PU coating exhibited the highest wear under reciprocating testing. From **Figure** 6.12(b), it can be observed that there was a 75 and 95% reduction in the specific wear volume with the addition of MoS_2 and MoS_2-ODT nanosheets, in the polymer matrix. It has been widely reported in the literature that the low wear of polymer materials is because of the material transfer to the countersurface, which forms a thin tribofilm [41,49,60,201,316,325,326]. However, the authors were not able to analyze the countersurface in the reciprocation tests as the size of the ball used for testing was quite small (5 mm), and the transfer layer used to get removed while removing the ball from the collet. The PU-MoS_2-ODT coating showed a better H/E ratio than the PU-MoS_2 coating. Hence showing better wear resistance. Moreover, the dispersion of MoS_2-ODT nanosheets was better than MoS_2 nanosheets (**Figure** 6.7(c) and (d)). Also, from **Figure** 6.11(a), it can be observed the running in time of PU-MoS_2-ODT coating is lesser than PU-MoS_2-ODT, indicating that the tribofilm forms at early stages in PU-MoS_2-ODT coating, which helps in reducing wear. The PU-MoS_2-ODT coating showed lower specific wear and friction even when tested at a higher load of 20 N. However, at 30 N, the coating showed significant fluctuations in friction and finally failed after 1000 seconds, and the same situation was observed with the plain PU and PU-MoS_2 coating at 20 N. This may be due to the high Hertzian contact stresses (**Table** 6.3) being exerted on the surface at higher loads, which was higher than the hardness of the coating obtained through nanoindentation. Hence the high stress broke the polymer bonds and the coatings failed. The friction and wear results show that PU-MoS_2-ODTcoating has better lubricating and load bearing property in boundary lubrication. **Figure** 6.13 compares the stereozoom and optical microscopic images of the wear scar of different coatings tested at 10 N load under reciprocating conditions. It is evident from the images that the polymers were subjected to varying degrees of damage. The plain

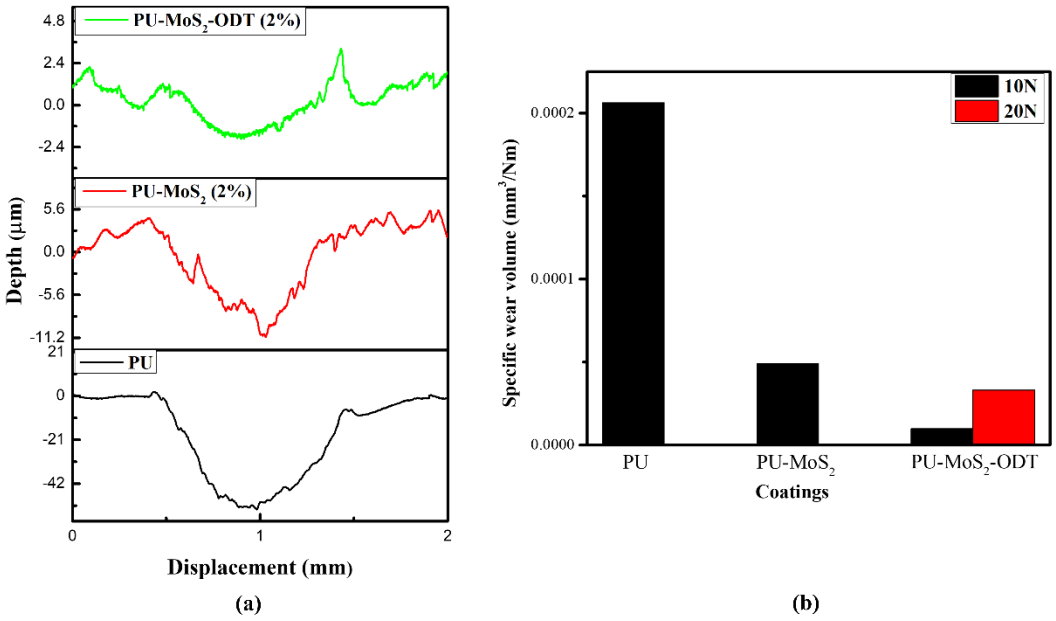

Figure 6.12. (a) Wear profiles of different coatings tested at 10 N in reciprocating testing, and (b) specific wear volume of different coatings at different loads (specific wear volume of the plain PU and PU-MoS_2 coating was not shown for 20 N, as these coatings failed during reciprocating tests).

PU coating (**Figure** 6.13(a)) shows severe plastic flow parallel to the sliding direction in the middle of the wear scar. Also, several deep grooves or cracks can be seen perpendicular to the sliding direction (**Figure** 6.13(d)). These cracks are characteristics of fatigue wear occurring because of repeated stress (loading and unloading) on the polymer surface, leading to the removal of a huge chunk of material from the surface. The PU-MoS_2 coating only showed some shallow cracks perpendicular to the sliding direction (**Figure** 6.13(e)), i.e., mainly comprising fatigue wear. At the same time, no signs of plastic flow were observed. The PU-MoS_2-ODT coating shows little signs of plastic flow and some abrasion marks in the sliding direction. Therefore, based on the above observation, it can be said that plastic flow and fatigue wear are the dominating wear mechanisms in PU based nanocomposite coatings, and the addition of MoS_2 nanosheets helped in a significant reduction in the wear.

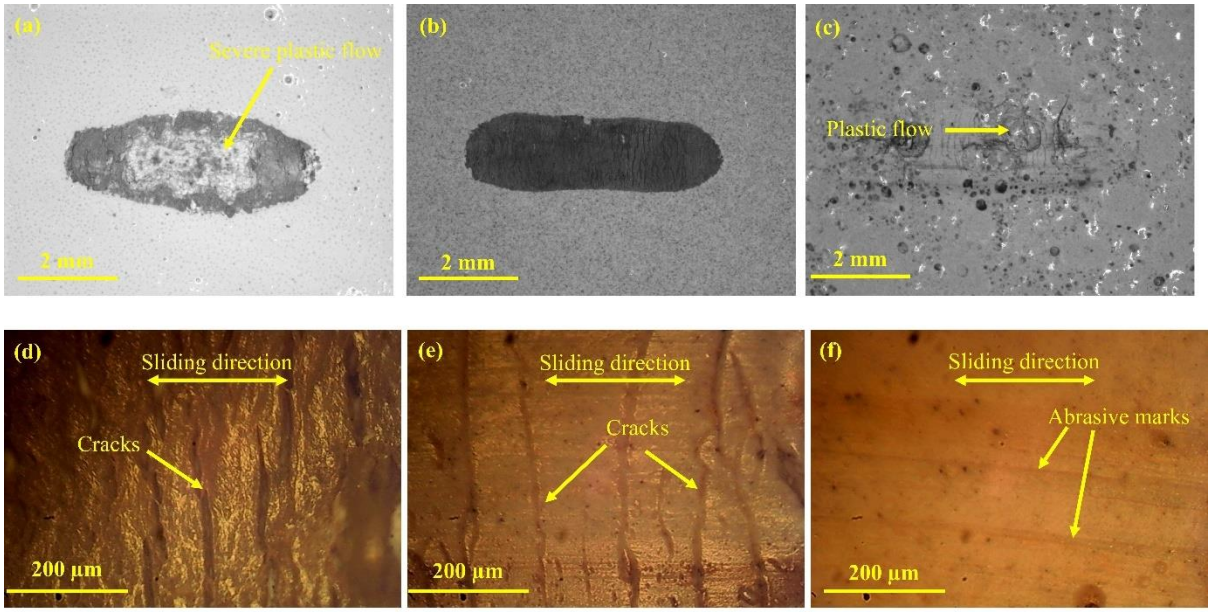

Figure 6.13. Stereozoom microscopic images of wear scar of (a) PU, (b) PU-MoS_2,and (c) PU-MoS_2-ODT coatings tested at 10N load. Optical microscopic images of wear scar of (d) PU, (e) PU-MoS_2, and (f) PU-MoS_2-ODT coatings tested at 10N load.

6.3.3.2. Galling tests of PU based nanocomposite coatings.

The friction torque values of various coatings at different degrees of applied stresses are shown in **Figure** 6.14**.** The occurrence of galling was identified by sudden fluctuations in the friction torque curves (marked with 'G'). From our previous investigation [250], it was established that the steel on steel tribopair galled at 5 MPa i.e., showed high fluctuations in friction torque within one rotation or 10 seconds. The plain PU coated samples, when tested against steel, didn't show any sudden rise in frictional torque value for 3600 seconds at 5 MPa. The samples were only tested for 3600 seconds as the mechanized galling test rig used for investigating the galling load is not designed to operate beyond 3600 seconds. According to ASTM G98 and ASTM G196, that load is considered where galling occurs within the first rotation. However, the plain PU coating did not fail after 360 rotations (rotational speed of 6 rpm). The plain PU coatings showed excellent galling resistance even at higher loads.

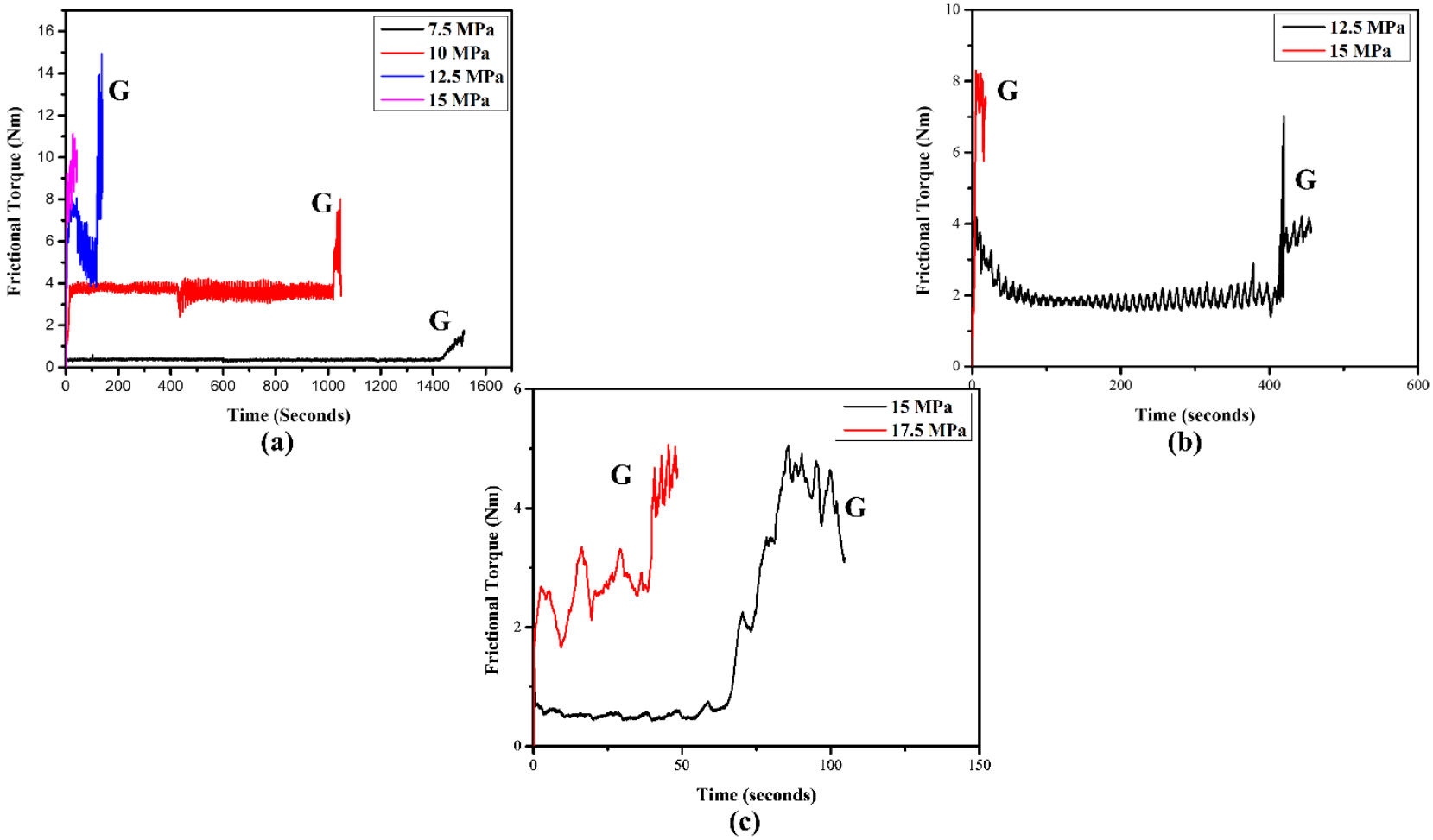

Figure 6.14. Friction torque curves of (a) PU, (b) Pu-MoS_2, and (c) PU-MoS_2-ODT coatings at various loads.

Figure 6.14(a) shows the frictional torque data of plain PU coating starting from 7.5 MPa. The plain PU coating galled after 1400 seconds (or 140 rotations) at 7.5 MPa. At 15 MPa, the plain PU coating galled within one rotation. The PU-MoS_2 coating also failed at 15 MPa within one rotation (**Figure** 6.14(c**)**), but the performance of coating at 12.5 MPa was better than plain PU coating. At the same time, the PU-MoS_2-ODT coating did not fail within one rotation, even at 17.5 MPa. The tests were not conducted at a higher load because of the limitation of the galling test rig, which can be tested up to 18 MPa. The friction torque values in PU-MoS_2 and PU-MoS_2-ODT coatings are relatively lower than the plain PU coating. This is attributed to the lubricating effect of MoS_2 nanosheets, which was also observed during reciprocating wear tests (**Figure** 6.11(a)). The stereozoom microscopic images in **Figure** 6.15 show the galled surfaces of the different coatings at different loads. After studying the galled surface of each coating, it was evident that the PU based coatings enhance the galling resistance by forming a thin tribofilm between the surfaces. All the images shown in **Figure** 6.15 are of the uncoated countersurface of SS 304 and PU based nanocomposite coated tribopair. Both the elements of the tribopair showed similar damage, and the microscopic images of the uncoated countersurfaces were studied to understand the anti-galling mechanism of PU based coatings. The uncoated counterfaces clearly show the transfer of tribofilm on its surface. The galling occurred in the areas where the tribofilm got removed. The tribofilm removal during galling testing started from the periphery of the sample (**Figure** 6.15(a) and (b)). This is because the maximum tangential velocity is near the circumference of the sample. Therefore, the shear force will also be maximum at the periphery of the surface. **Figure** 6.15(c) shows the SS 304 countersurface tested against PU-MoS_2-ODT coating. A smooth surface was found near the inner circle and the galled surface was at the outer circumference of the sample. The smooth surface was also because of the tribofilm, which protected the surface from wearing out during galling. The tribofilm got removed

Table 6.4. Number of rotations survived by different coatings before getting galled.

	5 MPa	10 MPa	15 MPa	17.5 MPa
Mo/DLC	4 rotations	3 rotations	Failure	-
PU	No failure till 360 rotations	17 rotations	Failure	-
PU-MoS_2	-	40 rotations	Failure	-
PU-MoS_2-ODT	-	-	5 rotations	4 rotations

while cleaning the surface for microscopic studies and hence cannot be seen in the image. The data given in **Table** 6.4 compares the number of rotations the galling samples survived in Mo/DLC multilayer coating (our previously published work [250]) with the PU based nanocomposite coatings used in the present literature at room temperature. In galling experiments, be it ASTM G98 or G196 , only that particular load is considered where the galling takes place within one rotation of the sample. So, both Mo/DLC coating and the plain PU and PU-MoS_2 coating fail at 15 MPa at room temperature. During galling testing, first the diffusion of the thin film takes place from the softer material to the harder countersurface. The adhered film is generally unstable and gets transferred back to the softer material, leading to small friction torque fluctuations. This period is also termed as the stable friction stage. After this stage, the diffusion rate between the hard and soft surfaces increases and significant fluctuations can be seen in the friction torque, which leads to the formation of lumps and scratches or plowing [269]. After observing the number of rotations sustained by coating before galling below 15 MPa, the PU and PU-MoS_2 coatings behaved better than Mo/DLC coatings, indicating that the thin transferred layer formed between the tribopairs is more stable than Mo/DLC coating. The MoS_2-ODT nanosheets not only decreased the coefficient of friction but also increased the hardness of the PU-MoS_2-ODT coatings. Hence the samples coated with PU-MoS_2-ODT coating were able to sustain higher loads during galling experiments and

showed good galling resistance at 17.5 MPa. The same kind of observation was also observed in reciprocating testing reported in the earlier section.

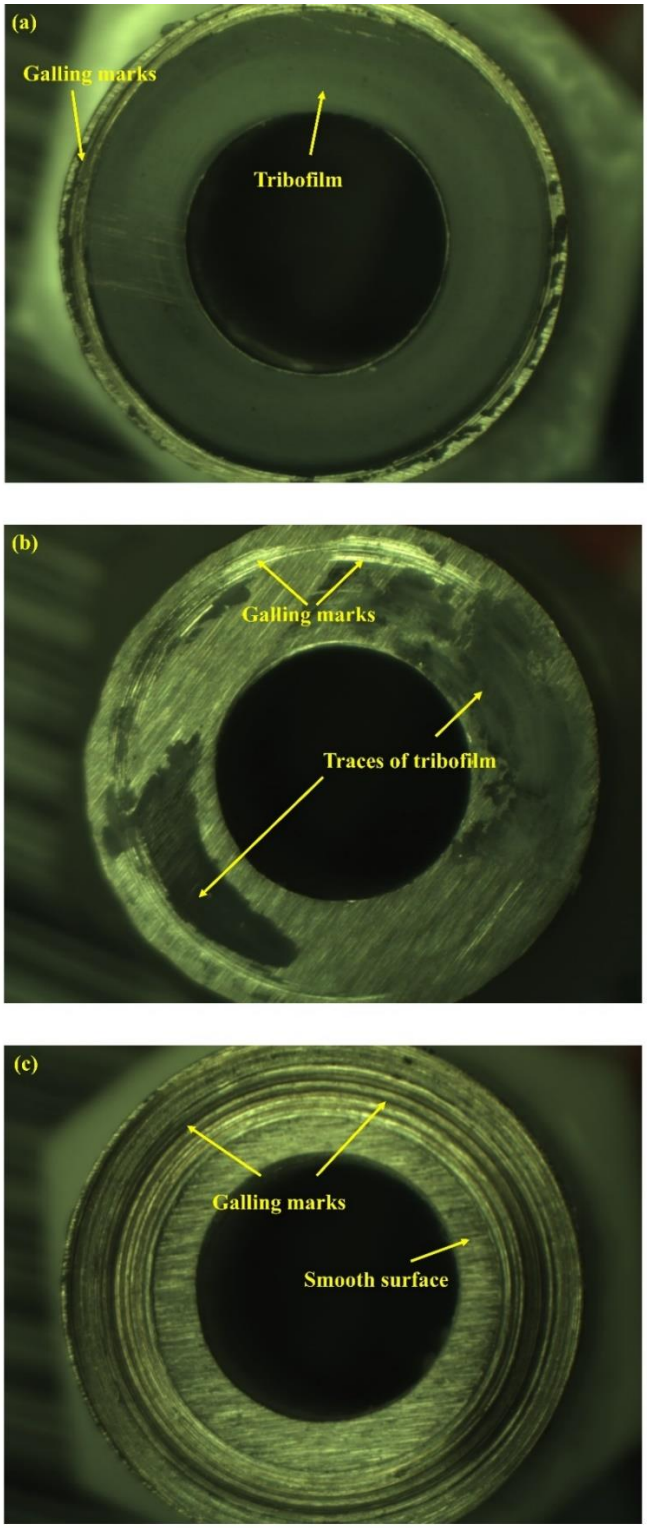

Figure 6.15. Stereozoom images of the galled surface of (a) plain PU coating at 10 MPa, (b) PU-MoS_2 coating at 12.5 MPa, and (c) PU-MoS_2-ODT coating at 17.5 MPa.

6.4. Summary.

The tribological (wear and galling resistance) properties of PU based coatings doped with (2 wt%) MoS_2 and MoS_2-ODT nanosheets were studied. The following conclusions can be drawn:

- The addition of MoS_2 and MoS_2-ODT nanosheets in the PU matrix decreased the surface energy, and enhanced the hardness, and H/E ratio (resistance of material towards elastic deformation) of the PU based coatings. This helped in a significant reduction in friction and wear of PU based coatings.
- The PU-MoS_2 coating observed 46 and 77% reduction in friction and wear, respectively. At the same time, the PU-MoS_2-ODT coating showed a 75 and 95% reduction in friction and wear, respectively.
- The functionalization of MoS_2 nanosheets with ODT helped in better dispersion of MoS2 nanosheets in the polymer matrix. It also decreased the surface energy of the coating due to its hydrophobic nature, which helped in better performance of PU-MoS_2-ODT coating than PU-MoS_2 coating.
- The MoS_2-ODT nanosheets did not show any remarkable performance compared to with MoS_2 nanosheets when mixed with lithium-based grease [213]. Whereas the MoS_2-ODT nanosheets showed a significant reduction in friction and wear than MoS_2 nanosheets under reciprocating sliding conditions when doped in PU matrix.
- The plain PU and PU- MoS_2 coating showed similar resistance to galling. MoS_2 nanosheets in PU- MoS_2 coatings showed lower friction torque values and sustained more rotations at 12.5 MPa, and both coatings failed within a single rotation (10 seconds) at 15 MPa.
- The coating with MoS_2-ODT nanosheets showed good resistance to galling even at 17.5 MPa. The formation of the transfer layer to the counter surface is easier in

polymers, which helped to improve the galling resistance of SS 304.

The PU based coatings do not possess the adhesive strength, hardness, and high temperature stability, unlike ceramic based coatings. As galling or cold working causes severe damage to SS 304 threads, nuts, tapped holes, and fasteners, the present investigation opens a new dimension of a cost-effective approach to enhancing galling resistance at room temperature of SS304 using polymer-based coatings.